Korean J. Chem. Eng., **27**(3), 999-1002 (2010)
DOI: 10.1007/s11814-010-0117-7

Optimization of inverted bulk heterojunction polymer solar cells

Bing Zhang*, Dong-Hyun Lee*, Heeyeop Chae*, Chinho Park, and Sung Min Cho*,***,†**

*School of Chemical Engineering, Sungkyunkwan University, Suwon 440-746, Korea
**School of Display & Chemical Engineering, Yeungnam University, Gyeongsan 712-749, Korea
***Advanced Materials and Process Research Center for IT, Sungkyunkwan University, Suwon 440-746, Korea
(*Received 6 August 2009 • accepted 14 September 2009*)

Abstract−We have successively fabricated inverted bulk heterojunction polymer solar cells employing ZnO and MoO_3 as electron and hole selective layers, respectively. The device structure is ITO/ZnO/P3HT : PCBM/MoO_3/Al. Differently from conventional polymer solar cells, ITO and Al work as electron and hole collecting electrodes in this inverted structure, respectively. We have found the optimal thickness of ZnO and MoO_3 to be 100 nm and 5 nm, respectively. The highest PCE was obtained to be 3.32% under AM 1.5 illumination at 1,000 W/m^2, which is the highest PCE of inverted solar cells reported previously in the literature.

Key words: Polymer Solar Cells, Invert Structure, Zinc Oxide, Molybdenum Oxide

INTRODUCTION

Organic photovoltaic (OPV) devices have attracted considerable interest as a promising low-cost alternative to inorganic-based photovoltaic devices [1,2]. The power conversion efficiency (PCE) of (polymer : fullerene)-based bulk heterojunction OPV devices has already reached higher than 5%. The high performance was achieved through the optimization of phase segregation in the polymer : fullerene blend and the development of new materials allowing better p-n interfaces and balanced charge transport [1-4]. Most of the OPV devices studied have been based on a conventional device architecture which consists of a poly(3,4-ethylenedioxythiophene) : poly(styrenesulfonate) (PEDOT : PSS) hole-transporting layer and a bulk heterojunction layer sandwiched between a hole-collecting transparent indium tin oxide (ITO) electrode and an electron-collecting metal electrode. The sequence of layers in the conventional bulk heterojunction OPV devices is ITO, PEDOT : PSS, active polymer : fullerene blend, and aluminum in the order from the bottom glass substrate. In the conventional structure, however, the degradation of ITO/PEDOT : PSS interface is inevitable because of the strong acidic nature of PEDOT : PSS [5-7]. To resolve these problems, many studies have been focused on searching alternative materials to the PEDOT : PSS layer in the inverted bulk heterojunction solar cell structure [5]. In inverted structure, the interface of ITO/PEDOT : PSS can be avoided, but instead new electron-selective and hole-selective layers are required. Previously, the inverted architecture with various electron-selective layers, Cs_2O_3 [8], TiO_x [9], and ZnO [5,10] was demonstrated. For the hole-selective layer, metal oxides with high work function such as MoO_3, V_2O_5, WO_3 have been demonstrated [5,11,12].

In this study, we report an efficient inverted OPV device with ZnO and MoO_3 as electron-selective and hole-selective layers, respectively. The optimal thicknesses of ZnO and MoO_3 layers are determined for maximizing PCE of the inverted OPV devices.

†To whom correspondence should be addressed.
E-mail: sungmcho@skku.edu

EXPERIMENTAL

The OPV devices were fabricated on patterned indium tin oxide (ITO) coated glass substrate (electrical resistance: 15 ohm/□), which was cleaned ultrasonically in TCE, acetone, methanol, and DI-water. For an electron-selective ZnO layer, a sol-gel derived zinc oxide precursor was spin coated after oxygen plasma treatment for 5 minutes. As a zinc source, zinc acetate ($Zn(O_2CCH_3)_2$) was utilized. The solvent and stabilizer used were 2-methoxy ethanol ($CH_3OC_2H_4OH$) and mono-ethanol amine (MEA, C_2H_7NO), respectively. The ZnO precursor was spin coated on top of ITO glass at 5,000 rpm for 30 s, and subsequently annealed to fabricate ZnO thin film at the temperature of 250 °C. To control the thickness of the ZnO layer, the spin coating process was repeated up to four times. For preparing the active layer, P3HT (poly(3-hexylthiophene), Rieke Metals. Inc.) and PCBM ((6,6)-phenyl C_{61} butyric acid methyl ester, Nano-C) were separately dissolved in chlorobenzene (Sigma-Aldrich) at 40 °C for 24 hours to give a final concentration of 20 mg/ml. The resulting solutions were then mixed at a 1 : 0.6 ratio (volume %) and ready for the spin coating. The active layer for the bulk heterojunction OPV devices was spin coated at 1,500 rpm for 30 seconds. On top of the active layer, MoO_3 and 100 nm-thick Al layers were subsequently deposited by the vacuum evaporation. The active area of the fabricated OPV devices was 0.09 cm^2. Finally, the fabricated devices were post-annealed at the temperature of 150 °C for 30 minutes in a nitrogen-filled glove box. The PCE measurement of the devices was carried out in ambient condition under white light illumination by AM 1.5 solar simulator (ABET Sun2000 Solar Simulator). The PCE values reported here are corrected for spectral mismatch but have not been certified.

RESULTS AND DISCUSSION

We have shown the device structure of inverted bulk heterojunc-

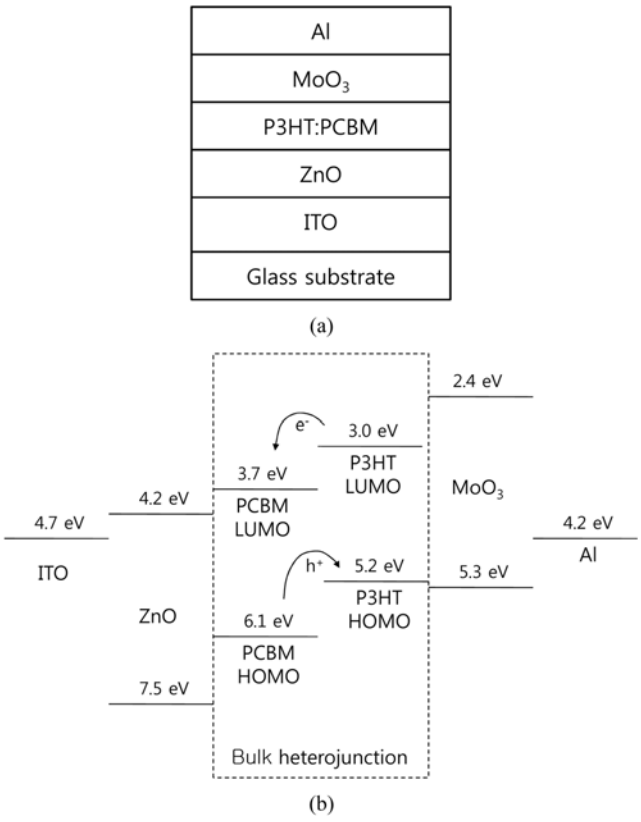

Fig. 1. (a) Structure of inverted organic solar cells fabricated in this study; (b) Energy level diagram for the inverted solar cells.

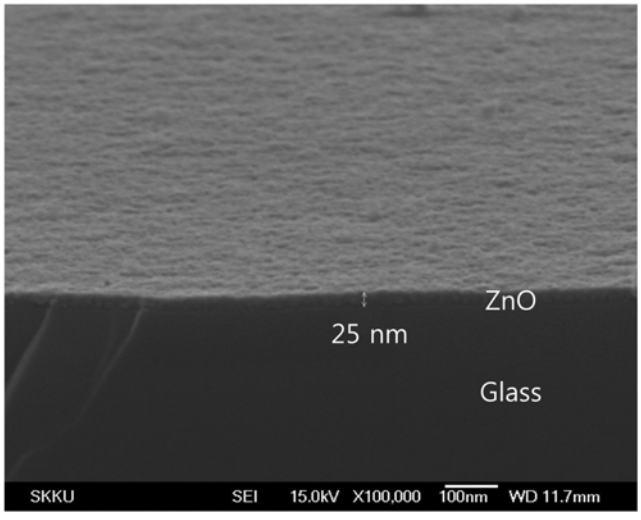

Fig. 2. Cross-sectional SEM image of sol-gel derived ZnO thin film on glass substrate.

tion polymer solar cell and the energy-level diagram of the device in Fig. 1. In the device, ZnO and MoO_3 layers were used as the electron and hole selective layers, respectively. For the invert structure solar cells, Cs_2O_3 [8], TiO_x [9] or ZnO [5,10] is usually used as the electron selective layer. In this study, we used ZnO as the electron selective material and the film was formed by spin coating with a sol-gel derived precursor. The surface morphology of grown ZnO

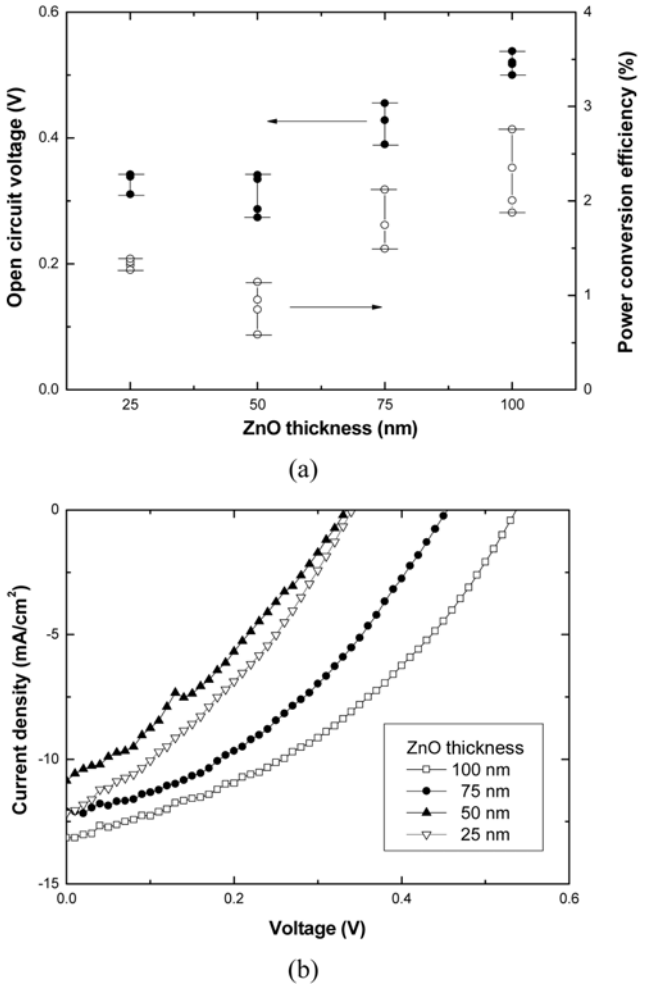

Fig. 3. (a) Effect of the thickness of electron-selective ZnO layer on V_{oc} and PCE; (b) I-V characteristics of devices with different ZnO thickness.

thin film is shown in Fig. 2. Since a spin coating step yielded 25 nm thick ZnO layer, the thickness was controlled by the repetition of the spin coating step. Even though we have not shown here, ZnO layer has been confirmed by EDX analysis.

As shown in Fig. 3(a), the open-circuit voltage and power conversion efficiency (PCE) increased as the thickness of ZnO layer increased. Four cells with the same ZnO thickness were fabricated and the measured performance was denoted as the error bars in Fig. 3(a). Even though the device with 100 nm thick ZnO layer showed the best average PCE, we did not fabricate a device with thicker ZnO layer since the device performance varied cell by cell. It can be noticed from the figure that the open-circuit voltages of the inverted solar cells were found lower than those of the conventional solar cells. Even though they increase as the thickness of ZnO layer increases, the values are always below 0.6 V. We think that the low open-circuit voltage and poor fill factor are a typical characteristic of the inverted solar cells. Since we have utilized ZnO and MoO_3 layers in the devices, the mismatches in HOMO and LUMO levels of different layers could have caused the decrease in the open-circuit voltage. In Fig. 3(b), we show the I-V curves of the devices with ZnO layer of different thicknesses. In a series of experiment,

the thickness of the hole selective MoO_3 layer was fixed at 6.3 nm. Similar researches have been reported in the literature [5,13]. Kyaw et al. [5] reported the inverted solar cells with 120 nm thick ZnO and 15 nm thick MoO_3 layers, of which the highest PCE was 3.09%. They have utilized the bottom electrode of fluorine-doped tin oxide (FTO) and top metal electrode of silver (Ag) instead of ITO and Al used in this study, respectively. Tao et al. [13] reported the optimal condition for MoO_3 and top metal layers. They found that the highest PCE of 2.57% was obtained with 1 nm thick MoO_3 layer and Ag top contact. When Al was used as the top metal, the optimal thickness of MoO_3 layer was found 5 nm to give the PCE of 2.02%. In their study, nanocrystalline TiO_2 was utilized as the electron selective layer instead of ZnO. Even though it is difficult to compare directly the device performance of the aforementioned two studies due to the different electron selective materials used, it is useful to determine the optimal thickness for the hole selective MoO_3 layer.

MoO_3 layer has dual functions, which are hole transporting and electron blocking. MoO_3 has been utilized as a hole injection layer for organic light emitting diodes (OLEDs) [14,15] and a replacement of PEDOT : PSS (poly(3,4-ethylene-dioxythiophene)-poly-(styrenesulfonate)) in conventional organic solar cell [16]. Therefore, not only does MoO_3 have good hole transporting property but it also serves as an electron blocking layer because the conduction band of MoO_3 (2.4 eV) is much higher than the lowest unoccupied molecular orbital (LUMO) of the acceptor (3.7 eV) and donor (3 eV) as shown in Fig. 1(b) [5]. For these reasons, the inverted solar cells without MoO_3 layer do not exhibit an appreciable PCE [5,13].

In this study, we fabricated inverted solar cells with three different thicknesses of MoO_3 layer of 3.8, 5.0, and 6.3 nm, while the thickness of ZnO was fixed at 100 nm. We have shown the dependence of the open circuit voltage and PCE on the MoO_3 thickness in Fig. 4(a). As can be seen in the figure, the device with 5 nm thick MoO_3 layer showed the highest average open circuit voltage and PCE. We have also shown the I-V characteristics of the devices in Fig. 4(b). It should be mentioned here that the device with 5 nm MoO_3 layer showed an unusually high short-circuit current density over 15 mA/cm^2. From Figs. 3 and 4, it can be seen that the thickness of MoO_3 affected the short-circuit current density more severely than the thickness of ZnO did. We think that the MoO_3 layer works for collecting holes from the active layer effectively at the optimized thickness. Even though the high short-circuit current density is approaching a theoretical limit value, a similar value has been reported in the literature [18].

Finally, we have shown the performance of the optimized inverted solar cell in Fig. 5, along with that of the conventional organic solar cell. The conventional solar cell has the structure of ITO/PEDOT : PSS/P3HT : PCBM/Al and was fabricated by using chlorobenzene solvent [17]. The optimal thickness of ZnO and MoO_3 was found 100 nm and 5 nm, respectively. The highest PCE was measured 3.32% under AM 1.5 illumination at 1,000 W/m^2, which is the highest PCE of inverted solar cells reported previously in the literature.

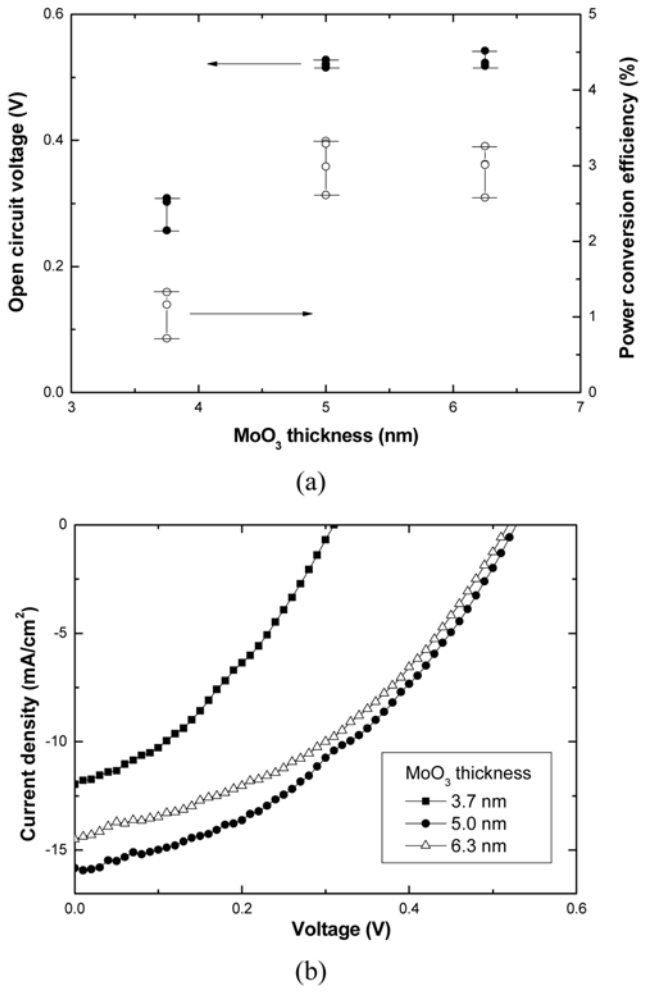

Fig. 4. (a) Effect of the thickness of hole-selective MoO_3 layer on V_{oc} and PCE; (b) I-V characteristics of devices with different MoO_3 thickness.

CONCLUSIONS

Invert structure polymer solar cells were fabricated with an MoO_3 hole selective layer and a sol-gel derived ZnO electron selective layer. The inverted structure was ITO/ZnO/P3HT : PCBM/MoO_3/Al. We have found the optimal thickness of ZnO and MoO_3 layers to be 100 nm and 5 nm, respectively. The highest power conver-

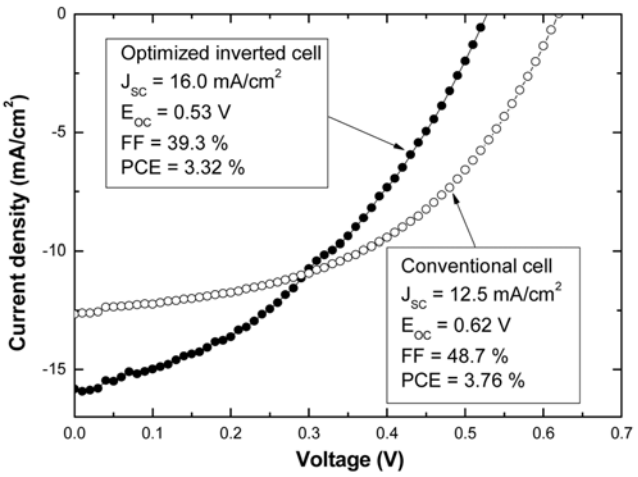

Fig. 5. I-V characteristics and device performance of an optimized inverted solar cell and conventional solar cell.

sion efficiency of 3.32% under AM 1.5 illumination at 1,000 W/m^2 was achieved with the optimized layer thickness.

ACKNOWLEDGMENTS

This work was supported by a grant from Gyeonggi Province through the GRRC (Gyeonggi Regional Research Center) program in Sungkyunkwan University.

REFERENCES

1. G. Li, V. Shrotriya, J. Huang, Y. Yao, T. Moriarty, K. Emery and Y. Yang, *Nat. Mater.*, **4**, 864 (2005).
2. M. L. Ma, C. Y. Yang, X. Gong, K. Lee and A. J. Heeger, *Adv. Funct. Mater.*, **15**, 1617 (2005).
3. J. Peet, J. Y. Kim, N. E. Coates, W. L. Ma, D. Moses, A. J. Heeger and G. C. Bazan, *Nat. Mater.*, **6**, 497(2007).
4. W. Y. Wong, X. Z. Wang, Z. He, A. B. Djurisic, C. T. Yip, K. Y. Cheung, H. Wang, C. S. K. Mak and W. K. Chan, *Nat. Mater.*, **6**, 521 (2007).
5. A. K. K. Kyaw, X. W. Sun, C. Y. Jiang, G. Q. Lo, D. W. Zhao and D. L. Kwong, *Appl. Phys. Lett.*, **93**, 221107 (2008).
6. M. P. de Jong, L. J. van Ijzendoorn and M. J. A. de Voigt, *Appl. Phys. Lett.*, **77**, 2255 (2000).
7. K. W. Wong, H. L. Yip, Y. Luo, K. Y. Wong, W. M. Lau, K. H. Low, H. F. Chow, Z. Q. Gao, W. L. Yeung and C. C. Chang, *Appl. Phys. Lett.*, **80**, 2788 (2002).
8. G. Li, C.-W. Chu, V. Shrotriya, J. Huang and Y. Yang, *Appl. Phys. Lett.*, **88**, 253503 (2006).
9. C. Waldauf, M. Morana, P. Denk, P. Schilinsky, K. Coakley, S. A. Choulis and C. J. Brabec, *Appl. Phys. Lett.*, **89**, 233517 (2006).
10. M. S. White, D. C. Olson, S. E. Shaheen, N. Kopidakis and D. S. Ginley, *Appl. Phys. Lett.*, **89**, 143517 (2006).
11. V. Shrotriya, G. Li, Y. Yao, C. W. Chu and Y. Yang, *Appl. Phys. Lett.*, **88**, 073508 (2006).
12. M. D. Irwin, B. Buchholz, A. W. Hains, R. P. H. Chang and T. J. Marks, *Proc. Natl. Acad. Sci.*, U.S.A., **105**, 2783 (2008).
13. C. Tao, S. Ruan, X. Zhang, G. Xie, L. Shen, X. Kong, W. Dong, C. Liu and W. Chen, *Appl. Phys. Lett.*, **93**, 193307 (2008).
14. S. Tokito, K. Noda and Y. Taga, *J. Phys. D.*, **29**, 2750 (1996).
15. H. You, Y. F. Dai, Z. Q. Zhang and D. G. Ma, *J. Appl. Phys.*, **101**, 026105 (2007).
16. V. Shrotriya, G. Li, Y. Yao, C. W. Chu and Y. Yang, *Appl. Phys. Lett.*, **88**, 073508 (2006).
17. B. Zhang, H. Chae and S. M. Cho, *Jpn. J. Appl. Phys.*, **48**, 020208 (2009).
18. C. Waldauf, P. Schilinsky, J. Hauch and C. J. Brabec, *Thin Solid Films*, **451-452**, 503 (2004).